

# RSC Advances



This is an *Accepted Manuscript*, which has been through the Royal Society of Chemistry peer review process and has been accepted for publication.

*Accepted Manuscripts* are published online shortly after acceptance, before technical editing, formatting and proof reading. Using this free service, authors can make their results available to the community, in citable form, before we publish the edited article. This *Accepted Manuscript* will be replaced by the edited, formatted and paginated article as soon as this is available.

You can find more information about *Accepted Manuscripts* in the [Information for Authors](#).

Please note that technical editing may introduce minor changes to the text and/or graphics, which may alter content. The journal's standard [Terms & Conditions](#) and the [Ethical guidelines](#) still apply. In no event shall the Royal Society of Chemistry be held responsible for any errors or omissions in this *Accepted Manuscript* or any consequences arising from the use of any information it contains.



## Remove of Chlorpyrifos from Waste Water by Wheat Straw-Derived Biochar Synthesized through Oxygen-Limited Method

Peifang Wang\*, Yayun Yin, Yong Guo\*, Chao Wang

Received 00th January 20xx,  
Accepted 00th January 20xx

DOI: 10.1039/x0xx00000x

www.rsc.org/

Systematic studies have been first time performed to investigate the pyrolysis behavior of wheat straw and the adsorption mechanism of chlorpyrifos by wheat straw-derived biochar. FTIR and elemental analysis results indicate that aromatic and hydrophobic substances are produced during the pyrolysis progress of wheat straw. BET results suggest that the pyrolysis temperature of wheat straw should be above 450 °C if one will acquire the biochar with surface area above 60.0 m<sup>2</sup> g<sup>-1</sup>. The adsorption experiments show that wheat straw-derived biochar at 750 °C (WS750) can effectively adsorb chlorpyrifos and the largest adsorption quantity is 16 mg/g. The driving force for chlorpyrifos adsorption by WS750 is most likely attributed to the π...π stack between the aromatic ring of chlorpyrifos and these aromatic areas on WS750 surface. The adsorption behaviors follow the pseudo-second kinetic and Freundlich models. Recycle experiments show that the adsorption ability of WS750 can be recovered by washing with methanol. The present work shows that wheat straw-derived biochar can work as a high effective and low cost adsorbent to remove chlorpyrifos from waste water.

### 1. Introduction

China is a large agricultural country since it has nearly the 1/4 of the world population to support. For making sure the high yield of crops, such as wheat and rice, pesticides have been widely used to kill pests. As a broad spectrum organophosphate pesticide, the toxicity of chlorpyrifos is lower than that of other organophosphate pesticides, such as meshamidophos and ammonium phosphate.<sup>1</sup> So, chlorpyrifos has been used to replace these highly toxic organophosphate pesticides for killing agricultural pests. However, it has reported that chlorpyrifos can transfer into river from farmland, which is toxic for some species in water, e.g. frog and fish.<sup>1</sup> Some methods have been developed to remove chlorpyrifos from water. Chishti et al used microorganisms to degrade chlorpyrifos in water.<sup>2</sup> Weston et al suggested that enzymes could be applied to evaluate and reduce the toxicity of chlorpyrifos in water.<sup>3</sup> TiO<sub>2</sub> was used to photodegrade chlorpyrifos in water by Kanmoni et al.<sup>4</sup> Adsorption is the commonly used method to remove these contaminants from water since of its simplicity and low cost.<sup>5</sup> Presently, most of researches focus on the adsorption and desorption of chlorpyrifos to soil.<sup>6</sup> Reports using adsorbents to remove chlorpyrifos from water are rare. Zhao et al<sup>7</sup> has found that the residual of drinking water treatment material can effectively adsorb chlorpyrifos in water with respect to

paddy soil, which contains iron, aluminium hydroxide minerals and humic materials. And, the largest adsorption quantity is about 1.2mg/g.<sup>7</sup> It is still necessary to develop low cost and high effective adsorbents for removing chlorpyrifos from waste water.

As a large agricultural country, the wheat yield in China is very high,<sup>8</sup> which leads to a large number wheat straw. The traditional way of treating wheat straw is to directly burn them in the field, which has resulted in serious air contamination.<sup>9</sup> For reducing environmental pollution and waste recycling, many methods have been developed to reuse wheat straw, in which using wheat straw to produce biochar is the promising one since biochar can be applied to soil remediation, carbon dioxide fixation and adsorbent due to its large surface area and high microporosity.<sup>10</sup> Usually, wheat straw is converted into biochar in anoxic condition under high temperature.<sup>11</sup> However, the cost is high since inert gas, such as nitrogen, is needed for keeping a anoxic condition during carbonization process. In addition, the requirement for gas tightness of muffle furnace is high as well. For lowering the cost and simplifying the carbonization procedure, oxygen-limited method has been developed to synthesize biochar, in which oxygen availability was restricted by using a cover to close feedback in crucible.<sup>12</sup> Junna et al has prepared biochar with oxygen-limited method by using aluminium foil to wrap wheat straw during heating process.<sup>13</sup> Using cover to close wheat straw in crucible may be a better method to keep an oxygen-limited condition than that of using aluminium foil since the former is easier to use in a large-scale, can withstand higher temperatures and has a

\* Address Key Laboratory of Integrated Regulation and Resource Development on Shallow Lakes, Ministry of Education, College of Environment, Hohai University, P.R. China. E-mail: [pfwang2005@hhu.edu.cn](mailto:pfwang2005@hhu.edu.cn); E-mail: [quoyong@hhu.edu.cn](mailto:quoyong@hhu.edu.cn).

† Electronic Supplementary Information (ESI) available: Regents, the FTIR, TEM, EDS and fitting results are provided. See DOI: 10.1039/x0xx00000x

60 better gas tightness. Furthermore, surface area is a very  
61 crucial parameter for evaluating the adsorption ability of  
62 biochar. So far, the relationship between surface area  
63 and pyrolysis temperature of wheat straw derived  
64 biochar has not been investigated.

65 Currently, the studies on wheat straw derived  
66 biochar focus on using them to remediate the  
67 contaminated soil, such as to immobilize chlorobenzenes  
68 in soil,<sup>14</sup> to replace peat in soilless substrates,<sup>15</sup> and to  
69 adsorb cadmium cations in soil.<sup>16</sup> Report using wheat  
70 straw derived biochar to remove chlorpyrifos from water  
71 has not been found.

72 Herein, a detailed research has been first time  
73 performed to investigate the relationship between  
74 surface area and pyrolysis temperature of wheat straw  
75 derived biochar synthesized through oxygen-limited  
76 method, in which oxygen availability is restricted by using  
77 a cover to close wheat straw in crucible and the  
78 temperature varies from 250 °C to 750 °C. Then, these  
79 as-prepared biochar are used to adsorb chlorpyrifos for  
80 evaluating their adsorption ability. The obtained results  
81 show that wheat straw derived biochar can effectively  
82 remove chlorpyrifos from water. This work is helpful to  
83 promote the application of wheat straw derived biochar  
84 to purify waste water.

## 85 2. Experimental Section

### 86 2.1. Preparation of biochar

87 Wheat straw was first washed to remove mud and  
88 other impurities attached on its surface, followed by  
89 drying at 80 °C for overnight. Then, the dried wheat straw  
90 was crushed into powder through a disintegrator and  
91 subsequent passed through a 20 mesh sieve. After that,  
92 the obtained wheat straw powder was filled to the full  
93 crucible and the volume of the crucible was 100 ml.  
94 Whereafter, the crucible was closed with cover and  
95 heated in furnace at 250 °C, 350 °C, 450 °C, 550 °C, 650 °C,  
96 and 750 °C for two hours, respectively. The heating rate  
97 was 10 °C/min. These acquired biochar samples were first  
98 washed with 1 mol/L HCl to remove soluble minerals, and  
99 followed by the washing with deionized water to neutral  
100 state. These as-prepared samples were named as WS250,  
101 WS350, WS450, WS550, WS650 and WS750, respectively.

### 102 2.2. Characterization of samples

103 The thermal stability of wheat straw was characterized  
104 by thermogravimetric analysis (Netzsch STA 449 F1  
105 Jupiter, Germany). The H/C ratio in WS750 was  
106 determined by elemental analysis on the elemental  
107 analyzer (vario EL II, Elementar, Germany). The Fourier  
108 transform infrared spectrum spectra of WS250, WS350,  
109 WS450, WS550, WS650 and WS750 samples were  
110 acquired using Nexus 870 FT-IR instrument (USA). The  
111 surface areas of WS250, WS350, WS450, WS550, WS650  
112 and WS750 samples were determined with HD88,  
113 ASAP2020 micropore analyzer (USA). The morphology of  
114 WS750 was investigated with JEM-2100 electron

116 microscope (Japan). Zeta potentials of WS750 at different  
117 pH were performed using the Zetasizer Nano ZS (UK).

118 The chlorpyrifos concentration was determined at a  
119 wavelength 300 nm using High Performance Liquid  
120 Chromatography (HPLC, Waters e2696, USA) with a UV  
121 detector (Waters 2489) and a column (Bridge, 5µm,  
122 4.6×150 mm C18). The used mobile phase was the  
123 mixture of methanol and water (90:10 V:V), and the flow  
124 rate was 1 mL·min<sup>-1</sup>. The temperature of column was kept  
125 at 25 °C. The injected sample volume was 100 µL and the  
126 retention time was 3.9 min.

### 127 2.3. Adsorption experiments

#### 128 2.3.1. Adsorption experiments of chlorpyrifos by WS250, 129 WS350, WS450, WS550, WS650 and WS750 samples

130 The solubility of chlorpyrifos in water is just 1.2mg/L.  
131 So, a stock solution of chlorpyrifos (2.5g/L) was first  
132 prepared by dissolving chlorpyrifos in methanol. The  
133 stock solution was diluted into a specific concentration  
134 with 0.005 mol/L CaCl<sub>2</sub> solution for the adsorption test.

135 2.5mg biochar sample was weighted and put into an  
136 EPA bottle and the bottle cap has teflon gasket. EPA  
137 bottle was purchased from Shanghai ANPEI Instrument  
138 Co. Ltd, China. Then, 0.80mg/L chlorpyrifos was filled into  
139 the EPA bottle, followed by rotation for 48 hours with the  
140 rotation rate (70 r/min) at room temperature under dark  
141 conditions. Three parallel experiments were performed  
142 for each biochar sample. After adsorption experiments  
143 were finished, the supernatants in these EPA bottles  
144 were taken for determining the adsorption effect with  
145 HPLC method.

#### 146 2.3.2. Adsorption isotherms of chlorpyrifos by WS750

147 A series of chlorpyrifos solutions with concentration  
148 ranged from 0.40 mg/L to 1.2 mg/L were prepared for  
149 investigating the adsorption isotherm of chlorpyrifos by  
150 WS750. The procedure of chlorpyrifos adsorption by  
151 WS750 was same as that mentioned in 2.3.1 section.

#### 152 2.3.3. Adsorption kinetics of chlorpyrifos by WS750

153 The procedure of chlorpyrifos adsorption by WS750  
154 was same as that mentioned in 2.3.1 section. The  
155 concentration of chlorpyrifos was 0.80mg/L. The samples  
156 were collected at time intervals of 0.5, 1, 2, 4, 6, 8, 10, 12,  
157 24, 36, 48, 60 and 72 hours of rotation.

#### 158 2.3.4. Adsorption experiment of chlorpyrifos by the 159 inorganic component in WS750

160 5.0g WS750 sample was put into crucible and was  
161 heated at 800 °C for two hours without cover. The ash in  
162 the bottom of crucible was collected for investigating its  
163 ability to adsorb chlorpyrifos. The adsorption procedure  
164 was same as that mentioned in 2.3.1 section.

#### 165 2.3.5. The effect of CaCl<sub>2</sub> concentration on the 166 adsorption of chlorpyrifos by WS750

167 The effect of CaCl<sub>2</sub> concentration on the adsorption of  
168 chlorpyrifos by WS750 was also investigated. The  
169 concentrations of CaCl<sub>2</sub> ranged from 0.005mol/L, 0.010  
170 mol/L, 0.050 mol/L to 0.100 mol/L in the diluted  
171 chlorpyrifos solution. The concentration of chlorpyrifos is

172 0.80 mg/L. The adsorption procedure was same as that  
173 mentioned in 2.3.1 section.

### 174 2.3.6. The pH effect on the adsorption of chlorpyrifos by 175 WS750

176 The effect of pH on the adsorption of chlorpyrifos by  
177 WS750 was investigated as well. The pH of the diluted  
178 chlorpyrifos solution was adjusted to 3.05, 4.15, 5.23,  
179 6.12 and 7.06, respectively. The concentration of  
180 chlorpyrifos is 0.80 mg/L. The adsorption procedure was  
181 same as that mentioned in 2.3.1 section. We did not  
182 consider the adsorption of chlorpyrifos by WS750 in basic  
183 condition since chlorpyrifos would be decomposed in  
184 basic condition.<sup>1,7</sup>

### 185 2.3.7. Recycle experiment for adsorption of chlorpyrifos 186 by WS750

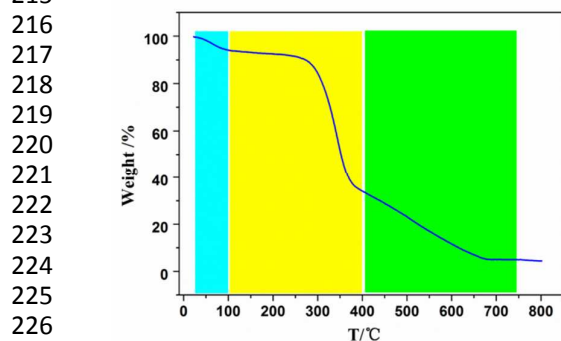
187 The adsorption procedure was same as that  
188 mentioned in 2.3.1 section. Three parallel experiments  
189 were performed for the adsorption of chlorpyrifos by  
190 WS750. After the adsorption experiment was finished,  
191 WS750 was collected and washed with methanol, then  
192 followed by the reuse of the collected WS750 to adsorb  
193 chlorpyrifos. This procedure was repeated three times.  
194

## 195 3. Results and discussion

196 A detailed analysis has been first performed to  
197 investigate the surface areas of these as-prepared  
198 biochar samples. According to Table 1, the pore volumes  
199 and pore diameters of WS250 and WS350 are not  
200 detected by micropore analyzer, suggesting that pore has  
201 not been formed in these two samples. Accordingly, the  
202 surface areas of WS250 and WS350 are just 0.114 m<sup>2</sup>g<sup>-1</sup>  
203 and 0.432 m<sup>2</sup>g<sup>-1</sup>, respectively. Then, the pore volumes  
204

205 Table.1 BET-N<sub>2</sub> Surface Area, Pore volume, Pore diameter,  
206 Ash Content and Yield of these as-prepared WS250-  
207 WS750 samples.

Biochar	T(°C)	BET (m <sup>2</sup> g <sup>-1</sup> )	Pore volume (cm <sup>3</sup> g <sup>-1</sup> )	Pore diameter (nm)	Ash (%)	Yield (%)
WS250	250	0.114	/	/	1.9	67.4
WS350	350	0.432	/	/	5.7	36.9
WS450	450	63.5	0.01	1.83	8.5	29.9
WS550	550	303	0.16	2.13	9.7	26.1
WS650	650	336	0.18	2.14	11	24.9
WS750	750	467	0.26	2.19	12	21.5



227 Fig.1 Thermogravimetric analysis of wheat straw.

228

229 and pore diameters of WS450, WS550, WS650 and  
230 WS750 become larger with the increased pyrolysis  
231 temperature, and surface area increases from 63.5 m<sup>2</sup>g<sup>-1</sup>  
232 of WS450 to 467 m<sup>2</sup>g<sup>-1</sup> of WS750. One obvious increase of  
233 surface area can be found according to Table 1: it is  
234 between 350 °C and 450 °C, in which the surface area  
235 increases from 0.432 m<sup>2</sup>g<sup>-1</sup> to 63.5 m<sup>2</sup>g<sup>-1</sup>. This implies  
236 that a pyrolysis temperature of 450 °C at least is needed  
237 for using wheat straw to produce biochar with oxygen-  
238 limited method since a significant surface area can just  
239 be acquired when pyrolysis temperature is above 450 °C.  
240 As far as we know, this is first time to make a clear  
241 description about the relationship between the surface  
242 area and the pyrolysis temperature of wheat straw-  
243 derived biochar, which is helpful for researchers to  
244 choose an appropriate pyrolysis temperature to produce  
245 wheat straw-derived biochar with large surface area.

246 For deep understanding the relationship between  
247 surface area and pyrolysis temperature of wheat straw-  
248 derived biochar, a thermogravimetric analysis (TGA) has  
249 been performed to investigate the pyrolysis behavior of  
250 wheat straw. It has reported that the components of  
251 wheat straw are mainly lignin, cellulose and  
252 hemicellulose,<sup>17</sup> in which cellulose and hemicellulose are  
253 decomposed from 350 °C to 400 °C, while lignin will be  
254 decomposed at a higher temperature than 400 °C.<sup>17-18</sup>  
255 According to Fig.1, three weight loss intervals are found  
256 from the TGA curve of wheat straw. The first one ranges  
257 from 25 °C to 100 °C, which is from the loss of the  
258 adsorbed water in wheat straw. The second one starts  
259 from 100 °C to 400 °C, being due to the thermal  
260 decomposition of cellulose and hemicellulose.<sup>17-18</sup> The  
261 third one ranges from 400°C to 700 °C, being attributed  
262 to the thermal decomposition of lignin.<sup>17-18</sup> By comparing  
263 Table.1 and Fig.1, one can deduce that the thermal  
264 decomposition of cellulose and hemicellulose will result  
265 in the formation of pore, and is most likely responsible  
266 for the abrupt increase of surface areas from WS350 to  
267 WS450. Furthermore, the surface areas from WS450 to  
268 WS750 continue to increase with the increase of  
269 pyrolysis temperature, which may be from the  
270 contribution of the pyrolysis of lignin at the higher  
271 temperature than 450 °C. So, the TGA result of wheat  
272 straw accounts well for the observed surface area results  
273 of wheat straw-derived biochar samples.

274 FTIR analysis has been further applied to investigate  
275 the pyrolysis process of wheat straw (Fig. S1). The broad  
276 peak around 3412 cm<sup>-1</sup> and the peak at 2920 cm<sup>-1</sup> are  
277 from the vibrations of O-H and aliphatic C-H<sub>2</sub> groups,  
278 respectively, while the peak at 1573 cm<sup>-1</sup> is assigned to  
279 the vibration of the aromatic C=C bond.<sup>19</sup> According to  
280 Fig. S1, the peaks of 3412 cm<sup>-1</sup> and 2920 cm<sup>-1</sup> gradually  
281 disappear, while the peak of 1573 cm<sup>-1</sup> gradually appears.  
282 This suggests that pyrolysis of wheat straw with the  
283 increased pyrolysis temperature will result in the  
284 formation of the aromatic and hydrophobic substances.  
285 In addition, the peak around 1100 cm<sup>-1</sup> in the FTIR curve

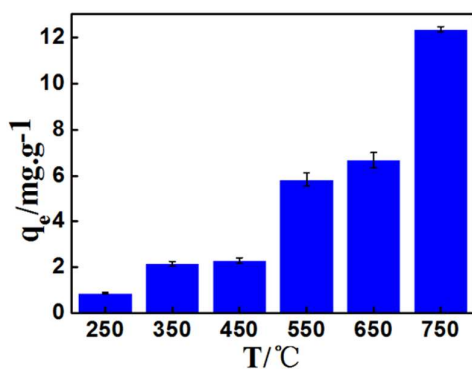


Fig.2 Comparison of chlorpyrifos adsorption by WS250-WS750 samples. The concentration of chlorpyrifos is 0.80 mg/L.

of WS750 is from the contribution of C-O and C-O-C groups,<sup>19</sup> implying that there are still some oxygen-containing functional groups on the surface of WS750 sample.

Chlorpyrifos is a broad spectrum organophosphate pesticide, which is toxic for some species in water, e.g. frog and fish.<sup>1</sup> According to our knowledge, wheat straw-derived biochar has not been used to adsorb chlorpyrifos from waste water. Herein, we first investigate the solubility of chlorpyrifos in water since it does not easily dissolve in water. According to Fig. S2, chlorpyrifos can dissolve well in water when the concentration is smaller than 1.2 mg/L. So, the concentrations of chlorpyrifos in this work are all smaller than 1.2 mg/L for avoiding the possible self-aggregation of chlorpyrifos. Then, we compare the adsorption ability of WS250-WS750 samples for chlorpyrifos. Based on Fig.2, WS750 has the highest adsorption ability for chlorpyrifos in all samples (about 12 mg/g), being due to that the aromatic and hydrophobic degree of WS750 is highest among all samples and chlorpyrifos has an aromatic ring as well. Thus, WS750 is chosen as model compound of wheat straw-derived biochar and further studies have been performed to investigate the adsorption mechanism of chlorpyrifos by WS750.

Further characterizations about WS750 have first been done. According to the TEM image (Fig.S3), the structure of WS750 is loose and there are many pores on its surface, which is consistent with the surface area result of WS750 (Table.1). The ratio of H/C is usually used to characterize the aromatization degree of biochar sample. For example, the ratios of H/C between 0.13 and 0.37 all suggest that the biochar samples have highly aromatic structure.<sup>19</sup> The H/C ratio of WS750 is 0.25, supporting that the aromatization degree of WS750 is high, which is in line with the FTIR analysis result of WS750. The inorganic constituents in WS750 are analysed through EDS method as well. Based on Fig. S4, the contents of O (55%, weight percentage) and Si (34%) are significantly higher than the rest elements, such as Na (0.08%), Al(0.38%), K(1.1%), Ca (3.6%), S(1.4%) and P(1.1%), suggesting that the

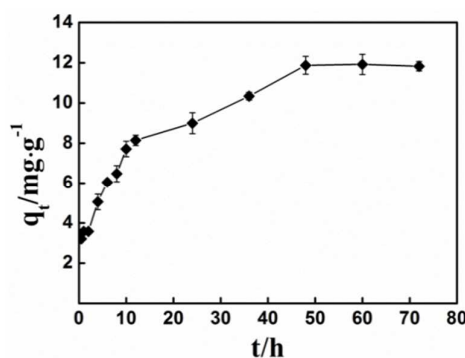


Fig.3 The chlorpyrifos adsorption by WS750 at 0.5, 1, 2, 4, 6, 8, 10, 12, 24, 36, 48, 60 and 72 hours, respectively. The concentration of chlorpyrifos is 0.80 mg/L.

inorganic constituent in WS750 is mainly SiO<sub>2</sub>.

The adsorption kinetics of chlorpyrifos by WS750 has been done by detecting the concentration of chlorpyrifos taken at 0.5, 1, 2, 4, 6, 8, 10, 12, 24, 36, 48, 60 and 72 hours, respectively. From Fig. 3, the adsorption of chlorpyrifos by WS750 includes two adsorption periods: fast adsorption and slow adsorption. Fast adsorption period is from 0 hour to 12 hours, and nearly 70% chlorpyrifos is adsorbed in this period. Slow adsorption period ranges from the 12 hours to 48 hours and the rest 30% chlorpyrifos is adsorbed. After 48 hours, the adsorption equilibrium arrives. Pseudo-first-order and pseudo-second-order models have been used to analyse the kinetic adsorption of chlorpyrifos by WS750 (Fig. S5 and Table. S1).<sup>20</sup> The experimental adsorption quantity of chlorpyrifos is 12mg/g, while the adsorption quantity of chlorpyrifos from pseudo-first-order model and pseudo-second-order model are 11.080±0.560mg/g and 12.195±0.593mg/g, respectively. Furthermore, the R<sup>2</sup> from pseudo-second-order model is 0.991, while the R<sup>2</sup> from pseudo-first-order model is 0.841. All of this suggest that the adsorption of chlorpyrifos by WS750 follows the pseudo-second-order kinetic. This implies that the adsorption sites on WS750 are not homogeneous, which are consistent with FTIR and TEM results. According to FTIR and BET results (Fig. S1 and Table.1), WS750 has aromatic surface and cavity with diameter larger than 2.19 nm. Fast adsorption is most likely from the adsorption of chlorpyrifos on the aromatic areas of WS750 surface and the mouth of the cavity in WS750. And the slow adsorption is possible from the transfer of chlorpyrifos from the mouth to the inside of the cavity.

The adsorption isotherm of chlorpyrifos by WS750 has been investigated as well. According to Fig. 4, the adsorption quantity of chlorpyrifos by WS750 increases with the increased concentration of chlorpyrifos, and the largest adsorption quantity is around 16 mg/g. Freundlich method is usually used to describe the adsorption behavior of biochar.<sup>21</sup> From Fig S6 and Table S2, the correlation coefficient R<sup>2</sup> is 0.968, implying that Freundlich method can describe well the adsorption

Journal Name

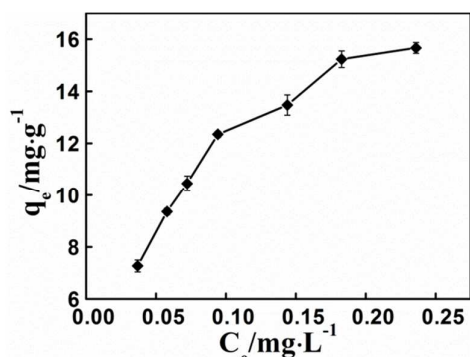


Fig.4 The adsorption isotherm of chlorpyrifos by WS750. The concentration of chlorpyrifos ranges from 0.40 mg/L to 1.2 mg/L.

behavior of chlorpyrifos by WS750. The  $K$  and  $1/n$  values from Freundlich fitting results are  $30.265 \pm 4.852$  and  $0.413 \pm 0.0187$ , respectively, implying that WS750 has strong affinity for chlorpyrifos. There is an aromatic ring in chlorpyrifos, and some areas on WS750 surface are aromatic. Thus, the affinity between chlorpyrifos and WS750 maybe from the  $\pi\text{-}\pi$  interaction between the aromatic ring of chlorpyrifos and these aromatic areas on WS750 surface.<sup>22-25</sup>

There is inorganic component in WS750 and EDS result has confirmed that the inorganic component is mainly  $\text{SiO}_2$ . An adsorption experiment has been performed to clarifying the role of the inorganic component in the adsorption of chlorpyrifos by WS750. The acquired result shows that the inorganic component in WS750 does not adsorb chlorpyrifos.

$\text{CaCl}_2$  has been added in the diluted chlorpyrifos solution for keeping a constant ionic strength.<sup>7</sup> Series adsorption experiments have been done to investigate the influence of  $\text{CaCl}_2$  concentration on the adsorption of chlorpyrifos by WS750. According to Fig. 5, the adsorption quantity of chlorpyrifos by WS750 decreases with the increased  $\text{CaCl}_2$  concentration. This may be due to that these increased ions ( $\text{Ca}^{2+}$  and  $\text{Cl}^-$ ) can occupy the adsorption sites on the surface of WS750 through ion-ion interaction,<sup>7, 24-25</sup> which leads to the decrease of chlorpyrifos

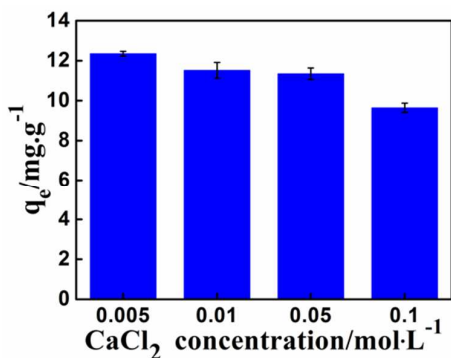


Fig.5 The influence of  $\text{CaCl}_2$  concentration on the adsorption of chlorpyrifos by WS750. The concentration of chlorpyrifos is 0.80 mg/L.

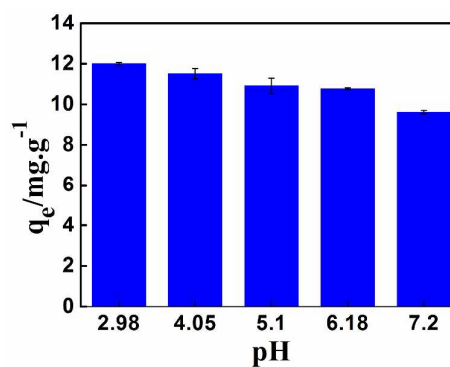


Fig.6 The influence of pH on the adsorption of chlorpyrifos by WS750. The concentration of chlorpyrifos is 0.80 mg/L.

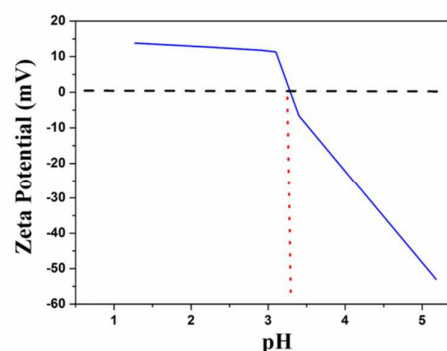
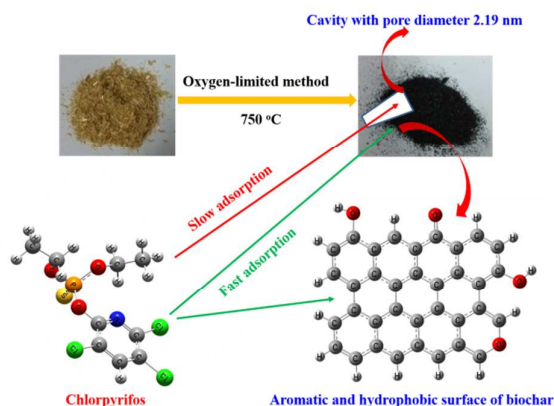


Fig.7 The surface charge of WS750 at different pH values.

adsorption.

A detailed adsorption experiments have also been performed to investigate the influence of pH on the adsorption of chlorpyrifos by WS750. According to Fig. 6, the adsorption quantity decrease with the increase of pH. For better understanding the experimental observation, the surface charge of WS750 at different pH has been investigated as well. The surface charge of WS750 at basic situation is not investigated since chlorpyrifos will hydrolysed at basic condition. Based on Fig. 7, the surface charges of WS750 change from positive to negative with the increase of pH from 1.27 to 5.18. The zero point charge of WS750 surface is around pH3.30. The change of charge on WS750 surface at different pH is most likely due to the protonation/deprotonation of oxygen-containing functional groups on WS750 surface. From Fig. S1, the peak around  $1100\text{ cm}^{-1}$  supports the existence of C-O and C-O-C groups.<sup>19</sup> In most of case, cation is most likely to interact with aromatic ring than anion.<sup>26-27</sup> So, it is easily to explain why WS750 with positive surface has a stronger adsorption for chlorpyrifos than that with negative surface. In addition, there are O atoms in chlorpyrifos. This means that the possible hydrogen bonding interaction between the proton on WS750 surface and O atoms in chlorpyrifos may also exist,<sup>23</sup> which will further increase the adsorption of chlorpyrifos by WS750 under low pH condition.

514 A possible adsorption mechanism has been proposed  
 515 to explain the adsorption behavior of chlorpyrifos by  
 516 WS750. FTIR, elemental analysis and BET results show  
 517 that some areas on WS750 surface are aromatic and  
 518 hydrophobic, while the diameter of cavity in the inside of  
 519 WS750 is about 2.19 nm. There is an aromatic ring in  
 520 chlorpyrifos and its size is less than 2.19 nm. Based on  
 521 the fitting results from Freundlich and pseudo-second-  
 522 order models, WS750 has strong attraction for  
 523 chlorpyrifos and the adsorption behavior include two  
 524 periods: fast adsorption and slow adsorption. From  
 525 Scheme.1,



530  
531  
532  
533  
534  
535  
536  
537  
538  
539  
540 Scheme.1 The possible adsorption mechanism of  
 541 chlorpyrifos by wheat straw derived biochar synthesized  
 542 through oxygen-limited method.

544 the  $\pi$ - $\pi$  interaction between the aromatic ring of chlorpyrifos  
 545 and the aromatic areas on WS750 surface may be responsible  
 546 for the effective adsorption of chlorpyrifos by WS750.<sup>22-25</sup>  
 547 Fast adsorption is most likely from the adsorption of  
 548 chlorpyrifos on the aromatic areas on WS750 surface and  
 549 the mouth of the cavity in WS750, while the slow  
 550 adsorption is possible from the transfer of chlorpyrifos  
 551 from the mouth to inside of the cavity.

552 The recycle adsorption experiments of WS750 have  
 553 also been performed to explore the possibility of using  
 554 WS750 as adsorbent to clean waste water in real  
 555 situation. The adsorption ability of WS750 is recovered  
 556 by washing with methanol. According to Fig. S7, the  
 557 adsorption quantity of WS750 decrease to 7.5 mg/g in  
 558 the second time from the 12 mg/g in the first time,  
 559 suggesting that washing can just recover the 63%  
 560 adsorption ability of WS750. Interestingly, the adsorption  
 561 ability of WS750 in the third time is nearly same as that  
 562 in the second time. According to Fig. 3 and Scheme.1, 70%  
 563 chlorpyrifos is adsorbed by WS750 in the fast adsorption  
 564 period. So, the chlorpyrifos adsorbed on WS750 surface  
 565 is easily to be washed by methanol, but the disadsorption  
 566 of chlorpyrifos in the cavity is not easily. However, the  
 567 adsorption quantity (7.5mg/g) is still higher than the  
 568 reported one (1.2mg/g),<sup>7</sup> and the recovery method is  
 569 very simple. So, it is feasible to use WS750 as adsorbent  
 570 for purifying waste water.

## 571 4. Conclusions

572 In summary, systematic studies have been performed  
 573 to investigate the pyrolysis behavior of wheat straw and  
 574 the adsorption mechanism of chlorpyrifos by wheat  
 575 straw-derived biochar. BET results suggest that the  
 576 pyrolysis temperature of using wheat straw to produce  
 577 biochar should be above 450 °C. FTIR and elemental  
 578 analysis support that the pyrolysis of wheat straw will  
 579 lead to the appearance of the aromatic and hydrophobic  
 580 substances. The adsorption experiments show that  
 581 WS750 can effectively adsorb chlorpyrifos and the largest  
 582 adsorption quantity is 16 mg/g. The driving force for  
 583 chlorpyrifos adsorption by WS750 is mainly from the  $\pi$ - $\pi$   
 584 interaction between the aromatic ring of chlorpyrifos and  
 585 the aromatic areas on the surface of WS750. Recycle  
 586 experiments show that the adsorption ability of WS750  
 587 can be recovered by washing with methanol. The present  
 588 work will be helpful to promote the application of wheat  
 589 straw-derived biochar to the purification of waste water.

## 590 Acknowledgements

591 Financial support was provided by the National Science  
 592 Funds for Creative Research Groups of China  
 593 (No.51421006), Program for Changjiang Scholars and  
 594 Innovative Research Team in University (No. IRT13061),  
 595 National Science Fund for Distinguished Young Scholars  
 596 (No. 51225901), the Fundamental Research Funds for the  
 597 Central Universities (2014B18614), Natural Science  
 598 Foundation of Jiangsu Province (SBK2015021389), A  
 599 Project Funded by the Priority Academic Program  
 600 Development of Jiangsu Higher Education Institutions.

## 601 Notes and references

- 602 ‡ Footnotes relating to the main text should appear here.  
 603 These might include comments relevant to but not central  
 604 to the matter under discussion, limited experimental and  
 605 spectral data, and crystallographic data.
- 606 1 D. L. Eaton, R. B. Daroff, H. Autrup, J. Bridges, P. Buffler,  
 607 L. G. Costa, J. Coyle, G. Mckhann, W. C. Mobley, L.  
 608 Nadel, D. Neubert, R. Schulte-Hermann, P. S. Spencer.  
 609 *Crit. Rev. Toxicol.* 2008, **38**, 1.
  - 610 2 Z. Chishti, S. Hussain, K. R. Arshad, A. Khalid, M. Arshad.  
 611 *J. Environ. Manage.* 2013, **114**, 372.
  - 612 3 D. P. Weston, C. J. Jackson. *Environ. Sci. Technol.* 2009,  
 613 **43**, 5514.
  - 614 4 V. G. G. Kanmoni, S. Daniel, G. A. G. Raj. *React. Kinet.*  
 615 *Mech. Catal.* 2012, **106**, 325.
  - 616 5 J. Zolgharnein, A. Shahmoradi, J. Ghasemi. *Clean-Soil,*  
 617 *Air, Water.* 2011, **39**, 1105.
  - 618 6 S.Y.Gebremariam, M.W. Beutel, D.R. Yonge, M. Flury,  
 619 J.B. Harsh. *Rev Environ Contam Toxicol.* 2012, **215**, 123.
  - 620 7 Y.Y. Zhao, C.H. Wang, L. A. Wendling, Y.S. Pei. *J. Agric.*  
 621 *Food Chem.* 2013, **61**, 7446.
  - 622 8 D. R. Wu, Q. Yu, C. H. Lu, H. Hengsdijk. *Europ. J.*  
 623 *Agronomy.* 2006, **24**, 226.
  - 624 9 X. H. Li, S. X. Wang, L. Duan, J. M. Hao, C. Li, Y. S. Chen,  
 625 L. Yang. *Environ. Sci. Technol.* 2007, **41**, 6052.
  - 626 10 J. J. Manyà. *Environ. Sci. Technol.* 2012, **46**, 7939.

## Journal Name

- 627 11 Y. Song, F. Wang, Y. R. Bian, F. O. Kengara, M. Y Jia, Z.  
628 B. Xie, X. Jiang. *J Hazard Mater.* 2012, **391**, 217.  
629 12 B. L. Chen, D. Zhou, L. Zhu. *Environ. Sci. Technol.* 2008,  
630 **42**, 5137.  
631 13 J. N. Sun, B. C. Wang, G. Xu, H. G. Shao. *Eco Eng.* 2014,  
632 **62**, 43  
633 14 Y. Song, F. Wang, F. O. Kengara, X. L. Yang, C. G. Gu, X.  
634 Jiang. *J. Agric. Food Chem.* 2013, **61**, 4210.  
635 15 S. F. Vaughn, J. A. Kenar, A. R. Thompson, S. C.  
636 Peterson. *Ind. Crops Prod.* 2013, **51**, 437.  
637 16 D. Y. Xu, Y. Zhao, K. Sun, B. Gao, Z. Y. Wang, J. Jin, Z. Y.  
638 Zhang, S. F. Wang, Y. Yan, X. T. Liu, F. C. Wu.  
639 *Chemosphere.* 2014, **111**, 320.  
640 17 M. I. Jahirul, M. G. Rasul, A. A. Chowdhury, N Ashwath.  
641 *Energies.* 2012, **5**, 4952.  
642 18 H. P. Yang, R. Yan, H. P. Chen, D. H. Lee, C.G. Zheng.  
643 *Fuel.* 2007, **86**, 1781.  
644 19 Q. L. Fang, B. L. Chen, Y. J. Lin, Y. T. Guan. *Environ. Sci.*  
645 *Technol.* 2014, **48**, 279  
646 20 F. Zhang, X. Wang, D. X. Yin, B. Peng, C. Y. Tan, Y. G. Liu,  
647 X. F. Tan, S. X. Wu. *J Environ Manage.* 2015, **153**, 68  
648 21 L. P. Lou, B.B. Wu, L. Wang, L. Luo, X.H. Xu, J. A. Hou, B.  
649 Xun, B. L. Hu, Y. X. Chen. *Bioresource Technol.* 2011,  
650 **102**, 4036  
651 22 C. X. Ren, L.X. Cai, C. Chen, B. Tan, Y.J. Zhang, J. Zhang.  
652 *J. Mater. Chem. A*, 2014, **2**, 9015  
653 23 M. À. Olivella, C. Bazzicalupi, A. Bianchi, N. Fiol, I.  
654 Villaescusa. *Chemosphere.* 2015, **119**, 863  
655 24 X. X. Chen, B. L. Chen. *Environ. Sci. Technol.* Article  
656 ASAP DOI: 10.1021/es5054946  
657 25 M. M. Watt, M. S. Collins, D. W. Johnson, *Acc. Chem.*  
658 *Res*, 2013, **46**, 955  
659 26 B. Sharma, H. K. Srivastava, G. Gayatri, G. N. Sastry. *J.*  
660 *Comput. Chem.* 2015, **36**, 529  
661 27 H. R. Masoodi, S. Bagheri, M. Mohammadi, M  
662 Zakarianezhad, B. Makiabadi. *Chem Phys Lett*, 2013,  
663 **588**, 31